Contribution on the kinematics of the polishing process on a polishing machine with horizontal overarm

Lukáš Veselý[1], *Ondřej* Matoušek[1, 2], *Tomáš* Vít[1, 3*], and *Miloš* Müller[3]

[1]asphericon s.r.o., 463 12 Jeřmanice, Czechia
[2]Technical university of Liberec, Institute of New Technologies and Applied Informatics, 461 17 Liberec, Czechia
[3]Technical university of Liberec, Dept. of Power Engineering Equipment, 461 17 Liberec, Czechia

Abstract. Understanding and controlling of the polishing process on conventional NC controlled machines is an important step to optimize production, reduce machine time and increase quality of production. The paper deals with the basic analysis of the problem and its comparison with the experiment performed during the real process on the machine and with the numerical MBS simulation of the process.

1 Polishing process

The technology of polishing of various materials is one of the oldest production processes. It therefore seems surprising that these processes are still not described by the corresponding analytical models, or a credible procedure for numerical simulations is not created. It is possible to find a number of publications that relate to individual partial problems of polishing. However, a comprehensive overview of procedures, supported by proper validation, is lacking. A closer look at the problem shows that the whole process is affected by a number of parameters, some of which are random in nature.

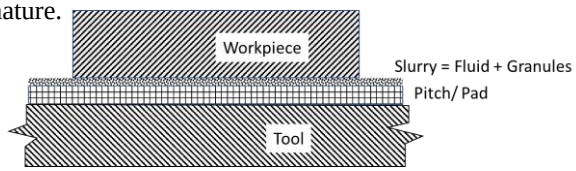

Fig. 1. Basic components of the polishing process.

In [1] it is possible to find a clear description of the components that are involved in the vast majority of polishing processes (see Fig. 1). The authors state that four most important components of the polishing chain include a workpiece, in our made from optical glass, fluid which represents the chemical composition of demineralized water and additives like pH controllers, inhabitants to control chemical interactions and surfactants.

The third main component of the polishing process are solid granules. Solid granules act together with the fluid component of polishing slurry. The task of the granules in the slurry is mainly the mechanical removal of material from the polished surface. The most important parameters of the granules are the chemical composition, size and shape of the individual particles and the concentration of the particles.

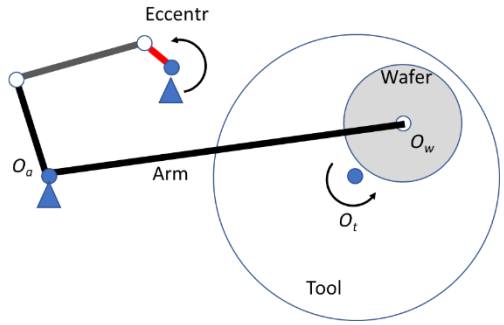

Fig. 2. Layout of NC polishing machine with horizontal overarm.

Fourth important part of the polishing chain is the polishing tool. The polishing tool provides relative motion between the granules and the workpiece. In most cases, the polishing tool consists of a rigid wall made of steel, alumina or silicon carbide, which serves as a carrier for a layer of pitch or various pads (polyurethane foam). Pads usually contain a variety of groove patterns to ensure even distribution of the polish slurry.

2 Kinematics of polishing

The basic arrangement of the polishing process is presented on Fig. 2. The tool rotation remains constant during the process, as does the shaft rotation, which transmits the speed to the eccentric arm of the lever mechanism. The oscillation of the arm and the associated speed of movement of the arm is thus determined by the geometric proportions of the individual arms.

The polished optical surface does not gain momentum per se. The only driving force of rotation is the rotational movement of the machining tool and movement of the arm. The kinematics of the polishing process without arm movement is very often described and analysed in the

* Corresponding author: tomas.vit@tul.cz

literature. For example, more detailed analysis of the problem is published in [2].

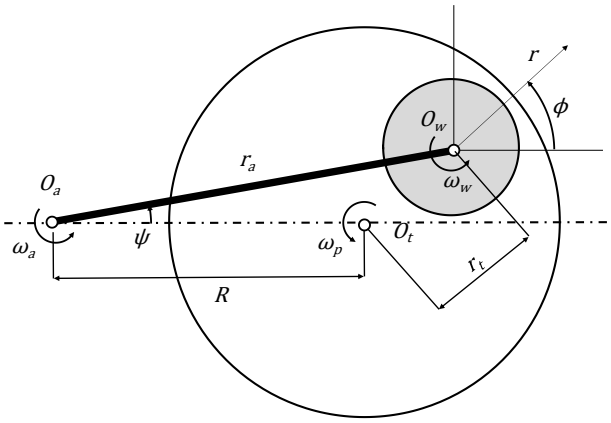

Fig. 3. Kinematics of the polishing mechanism.

Based on the kinematics of the horizontal overarm mechanism (Fig. 3) it is possible to separate the complex motion into three parts. Rotation of the workpiece, rotation of the polishing tool and motion of the arm. The resulting velocity correspond to the combination of the components mentioned above.

The velocity components of the workpiece (lens) in cylindrical coordinate system (r, ϕ) originated at the centre of the workpiece O_w are:

$$v_{w,r} = 0;\ v_{w,\varphi} = \omega_w r \tag{1}$$

Velocity components of the arm in the same coordinate system (r, ϕ) should be expressed as:

$$v_{a,r} = \omega_a r_a \sin\varphi\,;\ v_{a,\varphi} = \omega_a(r + r_a \cos\varphi) \tag{2}$$

and velocity components of the polishing tool as:

$$v_{t,r} = \omega_t r_t \sin\varphi\,;\ v_{t,\varphi} = \omega_t(r + r_t \cos\varphi). \tag{3}$$

Distance between centre of rotation of the workpiece and the tool should be expressed as $r_t = (R^2 + {r_a}^2 - 2Rr_a\cos\psi)^{1/2}$, where $R = |O_aO_t|$ denotes distance between rotation centre of the arm and the tool and $\omega_a = \frac{\delta\psi}{\delta t}$.

Components of the relative velocity should be expressed as:

$$v_{R,r} = \omega_a r_a \sin\varphi - \omega_t r_t \sin\varphi\,; \tag{4}$$

$$v_{R,\varphi} = \omega_w r + \omega_a(r + r_a\cos\varphi) - \omega_t(r + r_t\cos\varphi) \tag{5}$$

The magnitude of the relative velocity is:

$$v_R = \{[r(\omega_w + \omega_a - \omega_t) + \omega_a r_a \cos\varphi - \omega_t r_t \cos\varphi]^2 + [\omega_a r_a \sin\varphi - \omega_t r_t \sin\varphi]^2\}^{1/2} \tag{6}$$

The tangential component of viscous friction could be then written as:

$$dF_\varphi = \frac{\mu p(r\delta r\delta\varphi)[(\omega_a r_a - \omega_t r_t)\cos\varphi + r(\omega_w + \omega_a - \omega_t)]}{v_R} \tag{7}$$

And corresponding torque on the wafer:

$$M_w = \int_0^{r_w}\int_0^{2\pi} \mu p r^2 \left[\frac{(\omega_a r_a - \omega_t r_t)\cos\varphi}{v_R} + \frac{r(\omega_w + \omega_a - \omega_t)}{v_R}\right] d\varphi dr \tag{8}$$

It is obvious that for $\omega_w = \omega_t - \omega_a$ the torque of the wafer is $M_w = 0$.

In real operation, the connection between the arm and the workpiece body is realized via a ball joint. Additional torque is generated in the real process due to the friction in the ball joint. The moment M_w will therefore be nonzero and $\omega_w < \omega_t - \omega_a$.

3. Numerical simulation

Several approaches can be chosen for numerical simulation of the problem. Numerical simulation using tailored code requires detailed knowledge of the problem. On the other hand, it provides complete control over the progress of the solution, the resulting model is simpler and less demanding on computing power and time.

The use of commercial MBS systems enables very fast and user-friendly preparation of models. However, this is redeemed by the high computation time and the loss of control over the simulation process. Due to the complexity of the problem, this can lead to meaningless results.

We have chosen both approaches when solving this problem. However, custom code simulation is currently only applicable for polishing of flat surfaces

Fig. 4 shows the vector fields of the peripheral speeds of the tool (blue) and the workpiece (red).

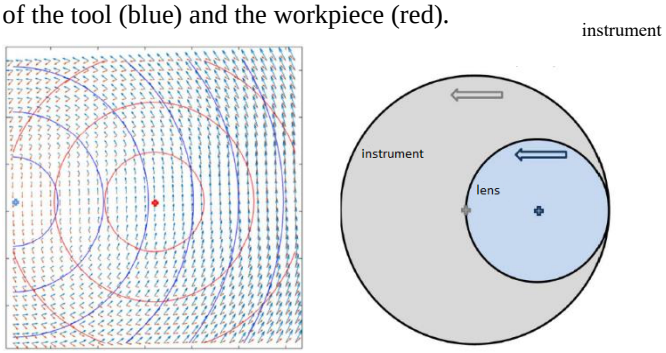

Fig. 4. Left, velocity vectors, blue color corresponds to tool, red to workpiece, crosses represent element centers, right, instrument and lens arrangement in Synchrospeed mode. The arrows indicate the direction of rotation.

Only the contact area of the tool and the polished surface is displayed. The red and blue contours, respectively, show the increasing circumferential speed of the workpiece and the tool, and it is clear from them how they overlap. The crosses of the respective colours show the centres of the individual elements. It is possible to get a good idea of the principle of the whole method from the direction of the individual arrows. If we focus on the development of velocities on the central axis, there is visible a clear development of circumferential velocities. At the centre of the tool, the circumferential speed is zero, but because the polished surface has its edge here, its circumferential speed is, on the contrary, maximum. As you move further along the axis, the circumferential speed of the workpiece decreases linearly, but the circumferential speed of the tool also increases linearly and the direction of movement of the surfaces is opposite in these positions.

Results from MBS simulation using Ansys Rigid Dynamics module are presented at Fig. 5 and Fig. 6. In contrast to the simulation in the MATLAB code, the beginning of the rotation of the tool in the time of 7 s and the associated transients is evident.

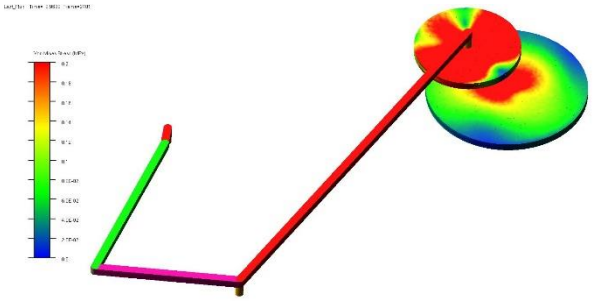

Fig. 5. MBS model of the polishing mechanism.

Presented results show the evolution of angular velocity as a function of time during polishing of planar surfaces. Due to the autorotational oscillating kinematics, the position of the polished surface is also time dependent.

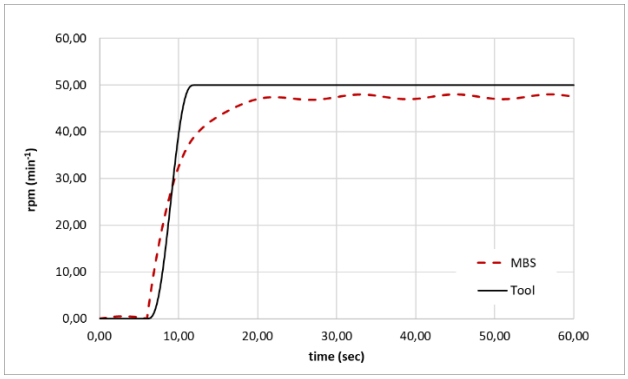

Fig. 6. results of MBS simulation.

4. Experiment

The whole experiment took place in a laboratory with a constant temperature of 24 °C. A 200 mm diameter tool with glued 0.58 g / cm^3 polyurethane was used on the NLP 400 HS-1. The density of the Auerpol PZ 110 polishing slurry used was 1.04 g/cm^3. To reduce the number of variables during polishing, the tool speed was set to a constant value of 50 rpm. Likewise, the rotation speed of the eccentric arm was set to a constant value of 5 rpm. The magnitude of the lens oscillation also remained unchanged throughout. The measurements were performed in eight positions of the tool relative to the workpiece $|r_a - R|$ = (-40; -30; -20; -10; 0; 10; 20; 30 mm). The positions are marked in Fig. 7.

However, only the results for $|r_a - R|$ = 30 mm are presented in this paper.

4.1. Measurement of the angular velocity of the workpiece

The position of the overarm was derived from acceleration measured by the accelerometer attached to the overarm. The signal was quite noisy due to vibrations generated during the sliding movement of the lens across the instrument (Fig. 8). It was necessary to perform a FFT to determine the frequency of the oscillating motion from the resulting frequency spectrum and to apply bandpass IIR filter to remove frequencieses generated by vibrations.

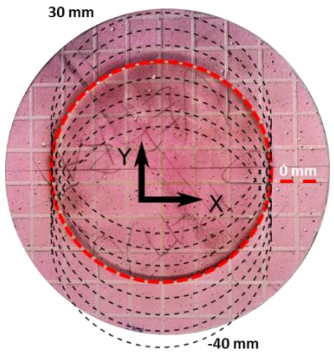

Fig. 7. Different Tool-Workpiece positions.

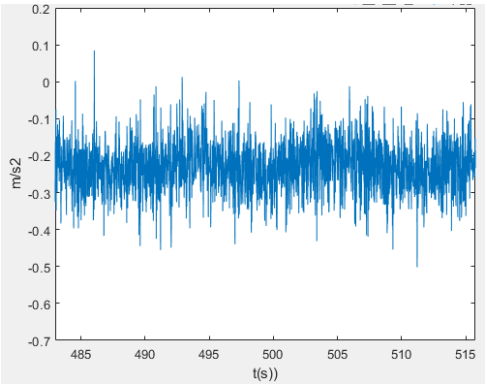

Fig. 8. Non processed results from angular velocity measurement.

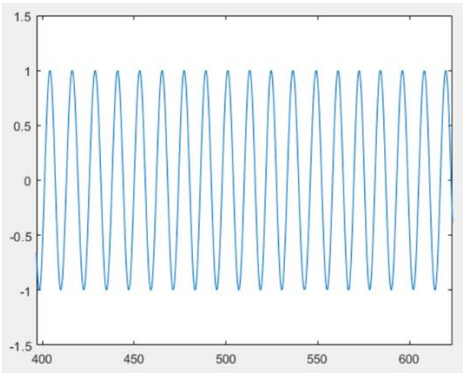

Fig. 9. Final filtered signal.

The Hilbert transform of the signal determined the waveform envelope function and removed the modulation. From an experimental point of view, only the relative position of the lens is important, so the loss of absolute position information due to modulation removal is irrelevant. The result of processed signal which shows relative position of the overarm as a function of time is presented in Fig. 9.

4.2. Measurement of the angular velocity of the workpiece

Angular velocity of the workpiece was measured by a non-contact optical sensor located in close proximity to the rotating workpiece. The workpiece was marked with tags and the time between the individual tags was evaluated during the experiment. From this, the angular velocity was subsequently evaluated.

From the theoretical assumptions and from the results of simulations, it is evident that the course of speed changes is sinusoidal. The frequency of the sine signal is given by the speed of rotation of the eccentric arm. The time period for the calculation was therefore chosen on the basis of the Nyquist criterion. After calculating the average speeds over the entire twenty-minute record, the appropriate data interpolation using the sine functions was performed.

Subsequently, a FFT analysis of the interpolated data (Figure 3) of the average angular velocity as a function of time was performed to confirm the results. This analysis showed the maximal amplitude at 0.0828 Hz, which corresponds to an eccentric arm rotation speed of 4.968 rpm.

5. Results

Fig. 10 shows comparison of the angular velocity achieved by different methods.

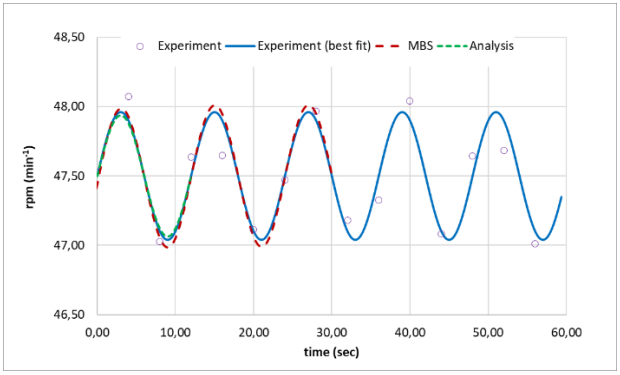

Fig. 10. Comparison of the achieved results.

It shows that different approaches could lead to comparable results. As it is difficult to determine the friction in the ball joint connecting the overarm and the workpiece the results from experiment were used to find this value. Presented comparison shows that results of analytical solution should be used for fast determination of the basic parameters of polishing process. However, the MBS is shown as powerful but expensive and time-consuming tool.

6. Conclusion

The nature of the rotational speed of the workpiece on conventional NC controlled machines can be determined by different methods, which give similar results. Results of analysis and numerical simulations are in agreement with results of precise experiments.

The rotational speed is given only by the transfer of force from the rotation of the tool to the lens. If the workpiece moves against the direction of tool rotation, the speed increases. On the contrary, when moving in opposite direction, the speed decrease.

Acknowledgements

The research has been supported by the Ministry of Industry and Trade, project The Country for the Future, FX01030046.

References

1. C. J. Evans, E. Paul, D. Dornfeld, D. A. Lucca, G. Byrne, M. Tricard, F. Klocke, O. Dambon, B.A. Mullany, CIRP Annals, Volume 52, Issue 2 (2003)
2. L. Jiun-Yu, Mechanics, mechanism and modeling of the chemical mechanical polishing process, Massachusetts institute of technology (2001)